OCT 19 1962

IS-538

Phase Diagram and Thermodynamic Properties* of the Yttrium-Zinc System

P. Chiotti, J. T. Mason and K. J. Gill

Institute for Atomic Research and Department of Chemistry

Iowa State University, Ames, Iowa

MASTER

ABSTRACT - Thermal, metallographic, and vapor pressure data were obtained to establish the phase boundaries and the standard free energy, enthalpy, and entropy of formation for the compounds in the yttrium-zinc system. Three compounds with stoichiometric formulas of YZn, YZn_2, and Y_2Zn_{17} melt congruently at 1105°, 1080°, and 890°C respectively. Four compounds with stoichiometric formulas of YZn_3, YZn_4, YZn_5, and YZn_{11} undergo peritectic reactions at 905°, 895°, 870°, and 685°C respectively. Three eutectics exist in this system with the following eutectic temperatures and zinc contents in wt pct: 875°C, 23.2 Zn; 1015°C, 51 Zn; 865°C, 82 Zn. The YZn_2 phase undergoes an allotropic transformation. In the two phase YZn_2-YZn alloys the transformation gives a weak thermal arrest at 750°C, whereas in the two phase YZn_2-YZn_3 alloys no thermal arrest is observed and the transformation occurs over a

---

*Contribution No. 1218. Work was performed in the Ames Laboratory of the United States Atomic Energy Commission.

temperature range below 750°C.

At 500°C the free energies of formation per mole vary from -18,090 for YZn to -53,430 for YZn_{11} and corresponding enthalpies vary from -24,050 to -92,080. The free energies and enthalpies per gram atom as a function of composition show a maximum for the YZn_2 phase; the 500°C values are -9,580 and -13,180 respectively.

INTRODUCTION

The only information found in the literature on yttrium-zinc alloys was the observation reported by Carlson, Schmidt and Spedding[1] that Y-20 wt pct Zn forms a low melting alloy. The alloy was produced by the bomb reduction of YF_3 and ZnF_2 with calcium in an investigation of methods for producing yttrium metal. The solubility of yttrium in zinc has been determined by P. F. Woerner[2] and reported by Chiotti, Woerner and Parry[3]. In the temperature range 495 to 685°C the solubility may be represented by the relation

$$\log_{10}N = -7663/T + 5.902$$

and in the temperature range 685 to 850°C by the relation

$$\log_{10}N = -4769/T + 2.946.$$

In these equations N represents atom fraction of yttrium and T is the temperature in degrees Kelvin.

The purpose of the present investigation was to establish the phase diagram for the yttrium-zinc system and to determine the standard free energy, enthalpy and entropy of formation for the compounds formed.

MATERIALS AND EXPERIMENTAL PROCEDURES

The metals used in the preparation of alloys were Bunker Hill slab zinc, 99.99 pct pure, and Ames Laboratory yttrium sponge. Arc-melted yttrium buttons contained the following impurities in parts per million: C-129, N-12, 0-307, Fe-209, Ni-126, Mg-13, Ca<10, F-105 and Ti<50. Some of the alloys containing 70 wt pct or more of zinc were prepared from yttrium containing 5000 ppm titanium as a major impurity.

Tantalum containers were found to be suitable for all alloys studied and were used throughout the investigation. The pure metals, total weight about 30 g, were sealed in one inch diameter tantalum crucibles by welding on preformed tantalum covers. A 1/8 inch diameter tantalum tube was welded in the base of each crucible for use as a thermocouple well. Welding was done with a heli-arc in a glove box which was initially evacuated and filled with argon. The sealed crucibles were enclosed in stainless steel jackets and heated in an oscillating furnace at temperatures up to 1150°C.

Homogeneous liquid alloys were obtained within a half hour at these temperatures except for alloys containing less than 20 pct zinc. The latter alloys were held at 1000-1100°C for two to three days in order to obtain equilibrium. After the initial equilibrations the tantalum crucibles containing the alloys were removed from the steel containers and used directly for differential thermal analyses. Further annealing heat treatments for alloys in which peritectic reactions were involved were carried out in the thermal analyses furnace. After thermal analyses the tantalum crucibles were opened and the alloys sectioned and polished for metallographic examination. In the following discussion alloys referred to as "quenched" were obtained by quenching the sealed stainless steel jacket containing the tantalum crucible and alloy in water.

The differential thermal analyses apparatus used was a modified version of the one described in an earlier paper[4]. The graphite crucible was replaced by an inconel crucible, the nickel standard and sample container were separated by a 1/8 inch MgO plate, no getter was used, and provisions were made to operate under an atmosphere of helium. This apparatus was checked against pure zinc and copper sealed

in tantalum crucibles. The melting points observed were within one degree of the accepted values. The dewpoint method and apparatus used in determining the zinc vapor pressure has also been described in an earlier paper[5].

EXPERIMENTAL RESULTS

Phase Diagram - The results of thermal analyses are summarized as open circles on the phase diagram, Fig. 1. The triangular points for the low temperature region of the zinc-rich liquidus represent solubility data obtained by Woerner[2]. Three eutectics and seven compounds were observed. The compositions of the eutectics in wt pct are 23.2, 51 and 82. The microstructures as well as thermal data indicate that the composition range of each compound is very limited and except for YZn and YZn_2 the compounds are represented on the diagram as line compounds. The microstructures of some of the alloys studied are shown in Figures 2-13. The etchants used were Nital (3 pct nitric in alcohol) and aqueous nitric acid solutions. The latter solutions were made by diluting a mixture consisting of two parts of a saturated solution of potassium tartrate and sodium fluosilicate and one part concentrated nitric acid. Figures 2, 3 and 4 show microstructures of an arc-melted button of yttrium, the 23.2 wt pct zinc eutectic

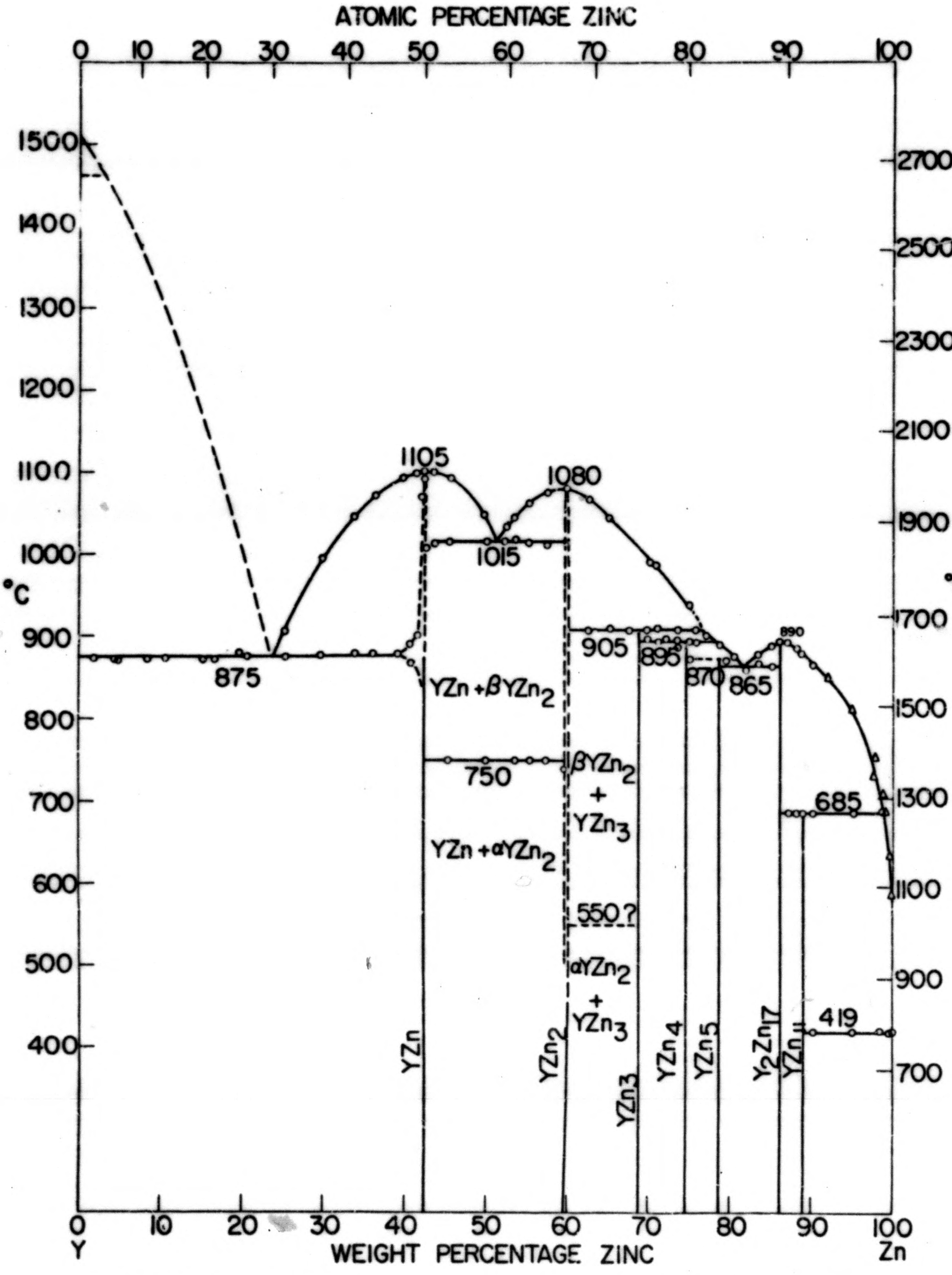

Fig. 1 - Phase diagram for the yttrium-zinc system under constrained vapor conditions.

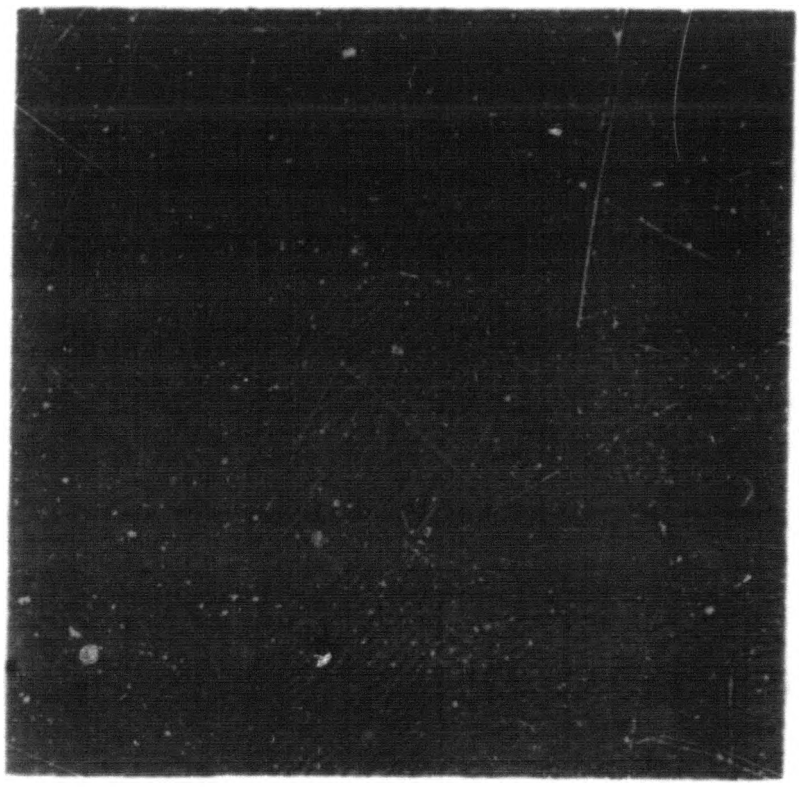

Fig. 2 - Arc-melted yttrium, X 150.

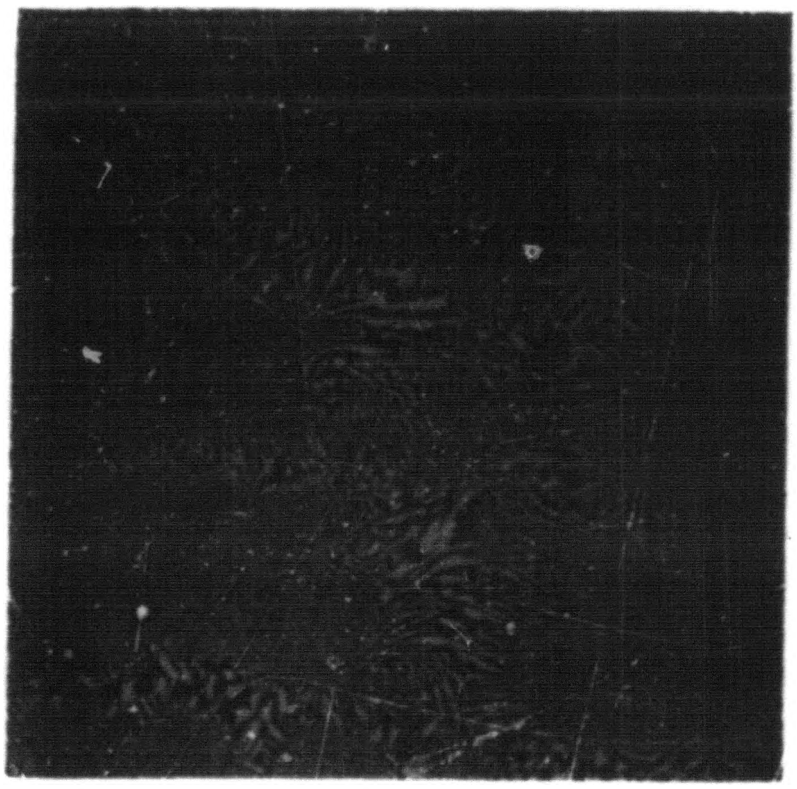

Fig. 3 - Y-23.2 wt pct Zn eutectic, furnace cooled, Nital etch, X100.

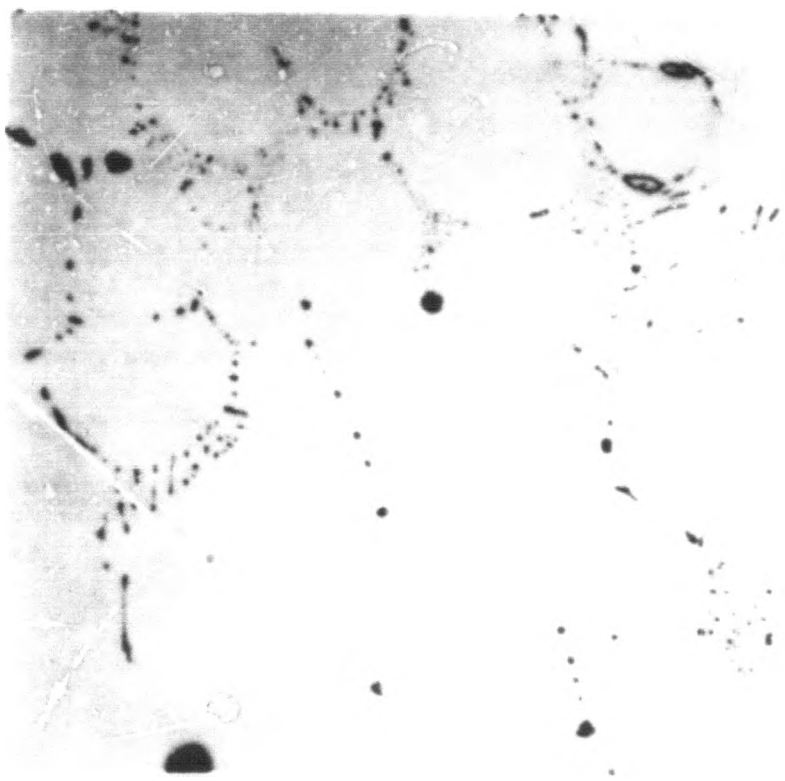

Fig. 4. Y-42.2 wt pct Zn annealed 48 hrs at 1000°C and quenched, HNO_3 etch, showing YZn with some segregation and pptn. of yttrium, X100.

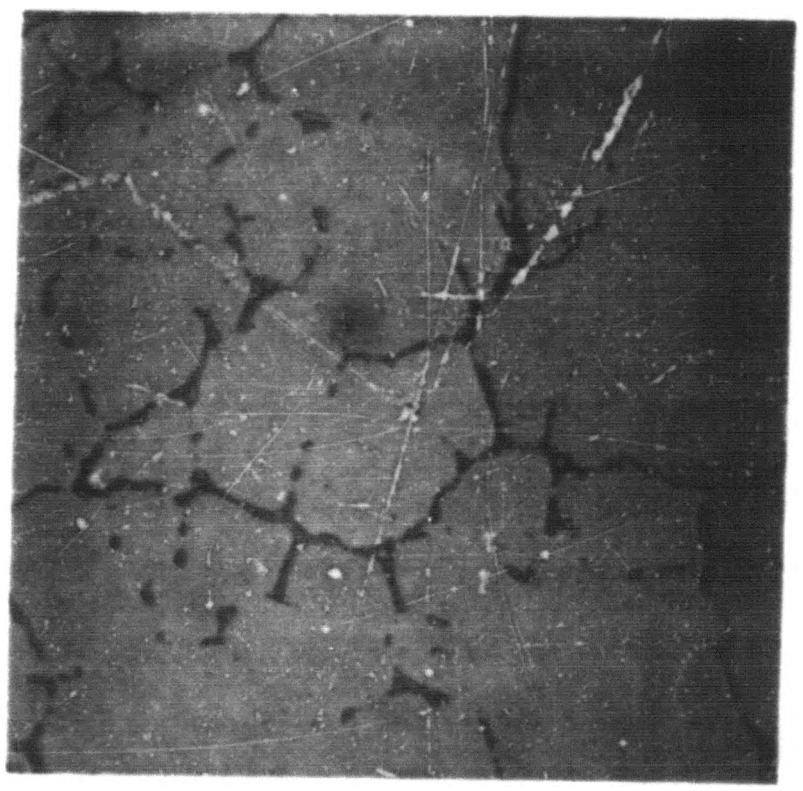

Fig. 5 - Y-58 wt pct Zn, annealed 100 hrs at 910°C and quenched, HNO_3 etch, showing YZn_2 with YZn grain boundaries, X100.

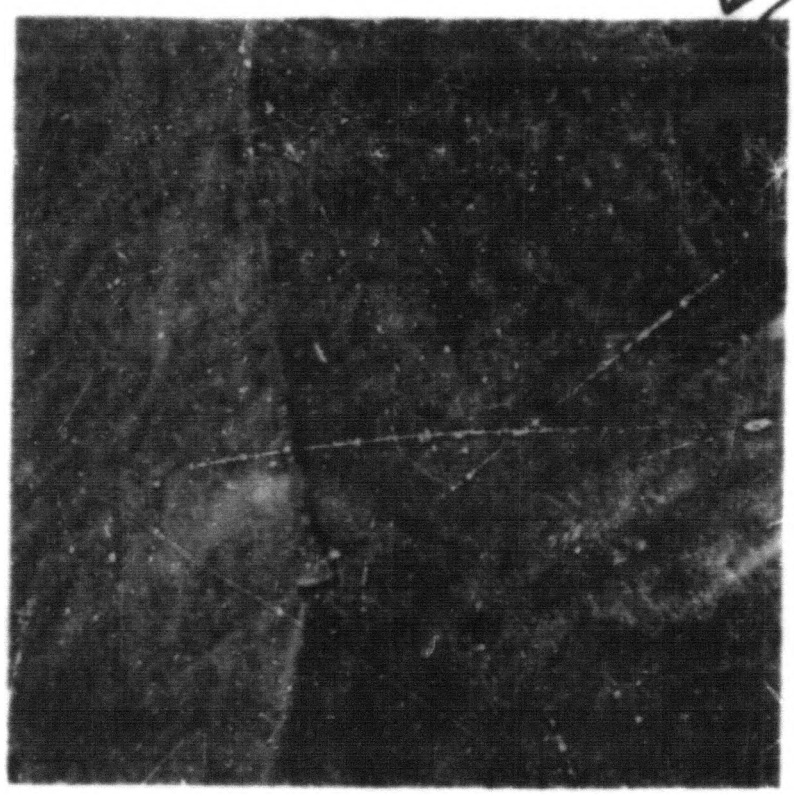

Fig. 6 - Same alloy as shown in Fig. 5 showing twinned structure of YZn_2, polarized light, X100.

Fig. 7 - Y-60.4 wt pct Zn, furnace cooled, showing acicular transformation structure of YZn_2, X500.

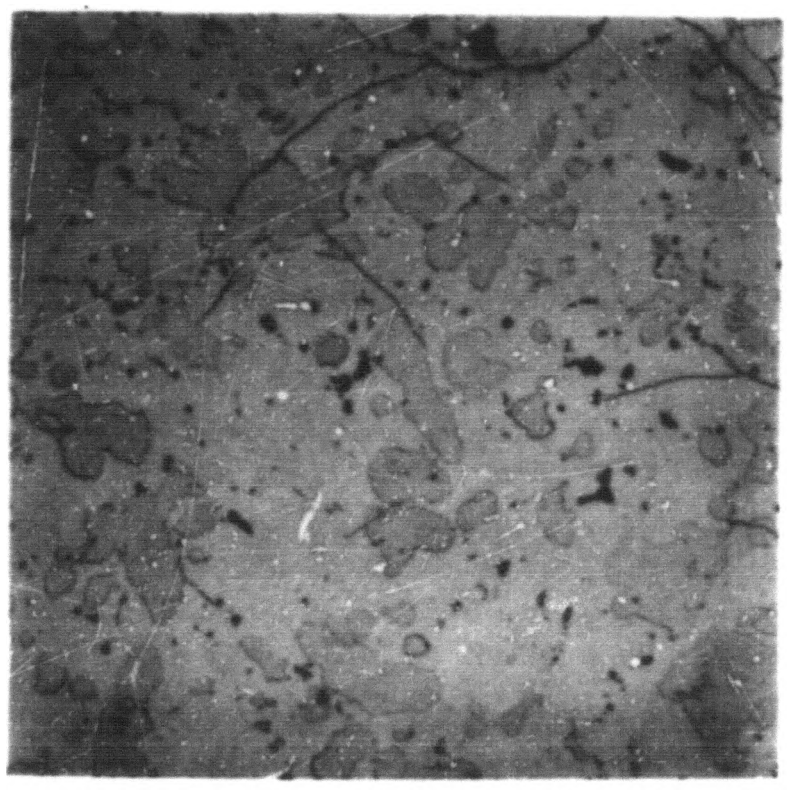

Fig. 8 - Y-67.0 wt pct Zn, furnace cooled, HNO_3 etch, showing YZn_2 dark phase in a YZn_3 matrix, X100.

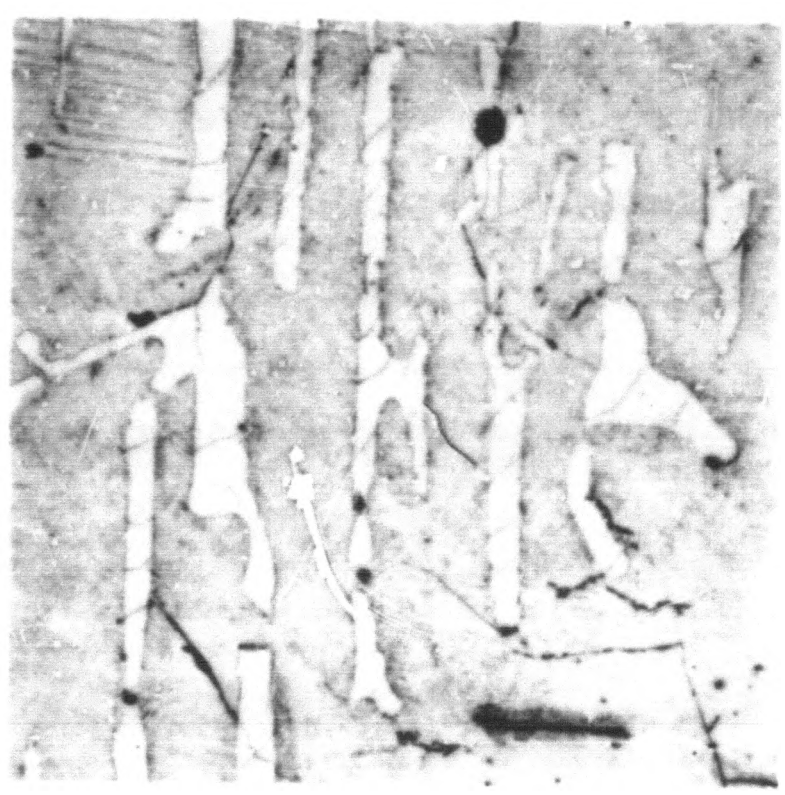

Fig. 9 - Y-74.9 wt pct Zn, furnace cooled, Nital etch, showing YZn_3, light phase, in YZn_4 matrix, X100.

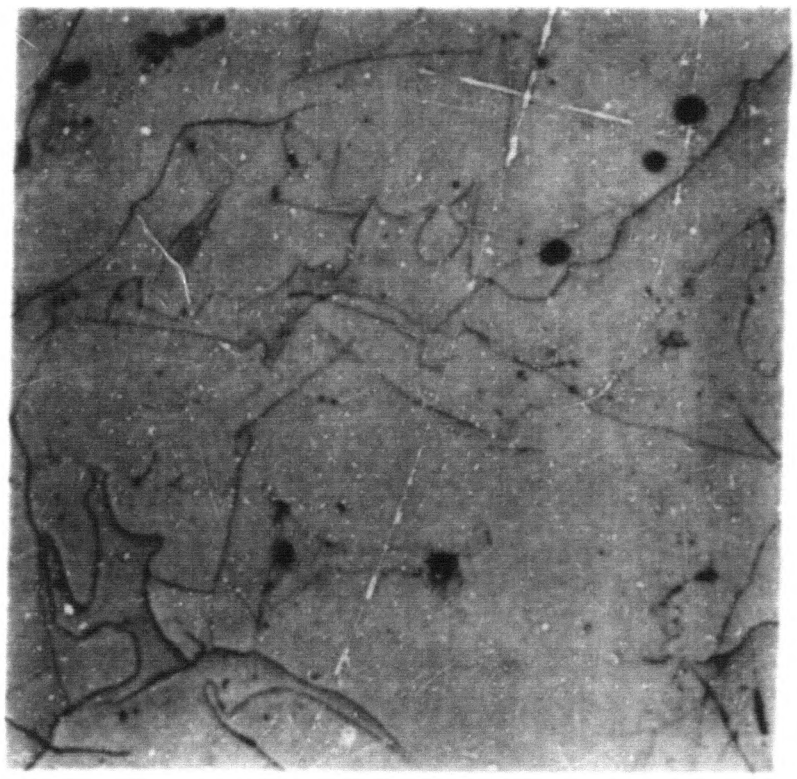

Fig. 10 - Y-78.6 wt pct Zn, furnace cooled, Nital etch, showing one phase YZn_5, X100.

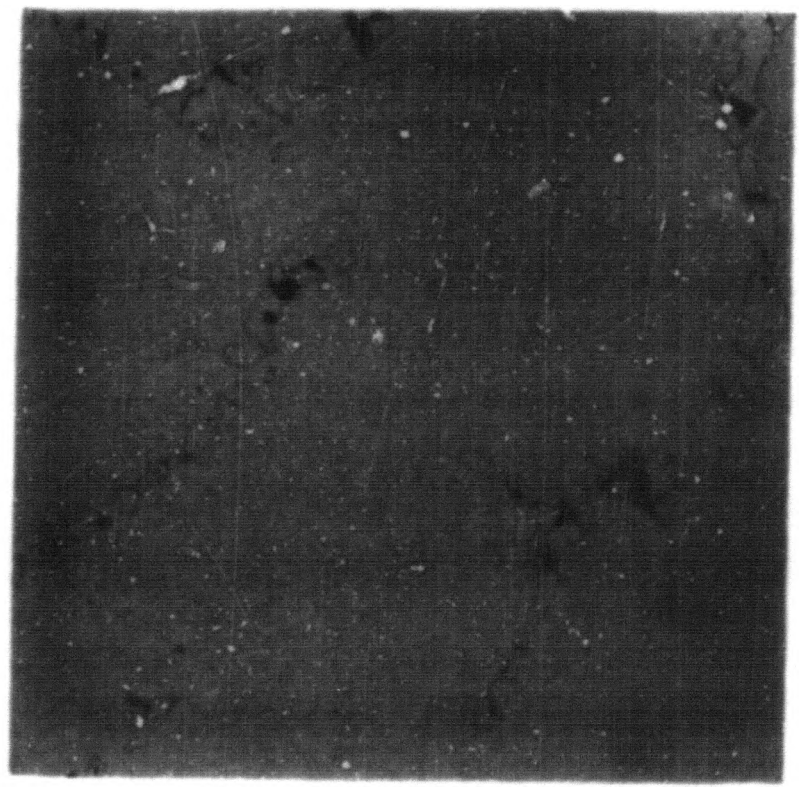

Fig. 11 - Y-86.2 wt pct Zn, furnace cooled, HNO_3 etch, showing YZn_{11} in Y_2Zn_{17} matrix, X100.

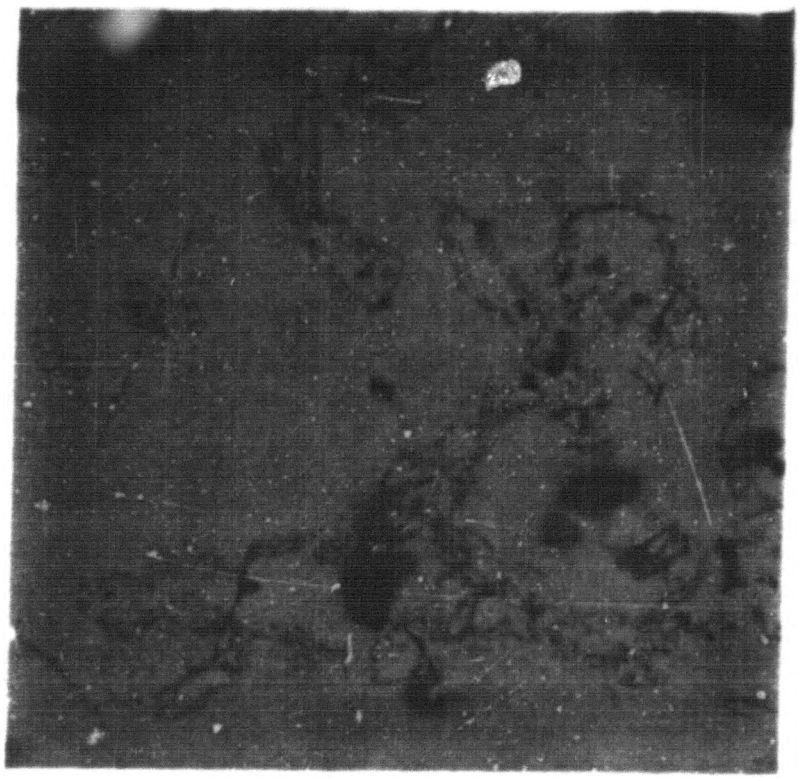

Fig. 12 - Y-87.9 wt pct Zn, annealed 100 hrs at 630°C, HNO_3 etch, showing Y_2Zn_{17} in YZn_{11} matrix, X100.

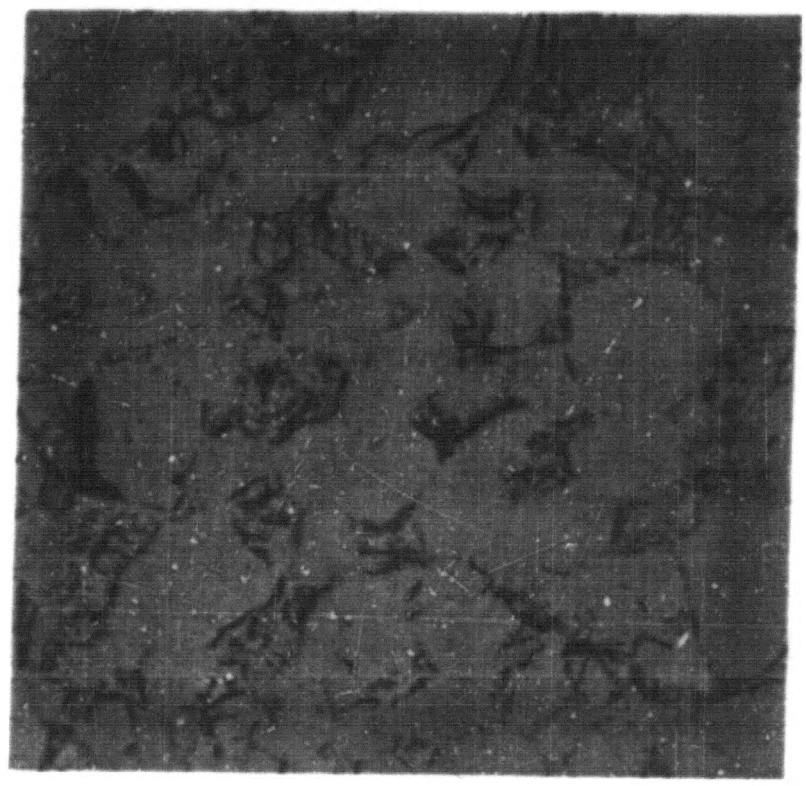

Fig. 13 - Y-91.9 wt pct Zn, annealed 100 hrs at 630°C, Nital etch, showing zinc in YZn_{11} matrix, X100.

and a 42.2 wt pct zinc alloy respectively. The latter alloy shows that the solubility of yttrium in the YZn phase (42.37 wt pct Zn) is very small at 1000°C. Thermal data indicate some solubility of yttrium in the YZn phase exists at near the eutectic temperature as shown on the phase diagram. The solid solubility of zinc in yttrium is very small. The lattice constants of yttrium in yttrium-rich alloys quenched from 1000°C showed only a very small increase over the lattice constants for the pure yttrium.

The compound YZn_2 undergoes an allotropic transformation. Alloys on the yttrium-rich side of YZn_2 give a definite but weak thermal arrest at 750°C on both heating and cooling. The microstructure of the YZn_2 phase shows a highly twinned structure, see Fig. 6. Alloys of composition corresponding closely to the stoichiometric composition of YZn_2 and of composition between YZn_2 and YZn_3 gave no thermal arrest at 750°C. Under bright field the YZn_2 phase shows a fine acicular microstructure, see Fig. 7. The YZn_2 phase in other alloys in this region, such as the alloy shown in Fig. 8, shows a highly twinned structure under polarized light similar to the structure shown in Fig. 6. Electrical resistance measurements made on alloys cast in 1/4 inch diameter tantalum tubes confirmed

the existence of a transformation in the YZn_2 compound. Alloys in the two-phase YZn-YZn_2 region show a discontinuity in the resistance at $750^{\circ} \pm 10^{\circ}C$. The electrical resistance of alloys in the YZn_2-YZn_3 composition range show that on cooling the transformation begins several hundred degrees below $750^{\circ}C$, is spread over a wide temperature range, exhibits sonic activity (clicks), and the resistance-temperature curve has a jagged saw-tooth shape. On heating no sonic activity was detected and the resistance-temperature curve is "S" shaped. This behavior is rather surprising in view of the very limited composition range for YZn_2.

Vapor Pressure and Thermodynamic Properties - The dew-point method was employed in measuring the zinc vapor pressure over a series of alloys with compositions representative of each of the solid two phase regions of the phase diagram. Alloys in which a peritectic reaction occurred on cooling from the molten state were annealed at temperatures below the peritectic temperature before dew point measurements were made. Alloys consisting of YZn_{11} and Y_2Zn_{17} phases were annealed at $630^{\circ}C$ for several days. Furnace cooled alloys in this composition range usually contained some unreacted zinc, which was evident in the microstructure. These alloys also gave a weak

thermal arrest at the freezing temperature for zinc. Annealing for 100 hrs at 630°C eliminated the zinc thermal arrest and no zinc was evident in the microstructure, see Fig. 12. Some zinc, dark areas in the YZn_{11} phase, is evident in the furnace cooled alloy shown in Fig. 11.

The vapor pressure of zinc over the alloys was calculated from the measured dewpoint temperatures and the known vapor pressure for pure zinc. Plots of the logarithm of the vapor pressure against the reciprocal of the absolute temperature were fitted to straight lines by a least squares treatment. The equations for these lines are summarized in Table I along with the temperature range of the measurements for each equation. In the case of alloys in the YZn-YZn_2 composition range a definite change in slope for the log P vs 1/T plot was observed at 750°C, the transformation temperature for YZn_2. These data were fitted to two curves, one for temperatures below 750°C for which alpha YZn_2 is one of the equilibrium phases and one for temperatures above 750°C for which beta YZn_2 is one of the equilibrium phases. No change in slope was observed at 750°C for alloys in the YZn_2-YZn_3 composition range. This discrepancy is believed to be due to the change in character of the alpha-beta transformation of

Table I. Zinc vapor pressure as a function of temperature for yttrium-zinc alloys

$$\text{Log}_{10}P_{atm.} = a/T + b$$

Equilibrium Phases	a	σ_s^*	b	σ_i^*	Temp. Range °K
Y-YZn	-11,510	69	7.02	0.07	905-1145
YZn-$\alpha$$YZn_2$	- 9,640	104	6.71	0.11	815-1020
YZn-$\beta$$YZn_2$	- 9,100	92	6.19	0.10	1020-1190
βYZn_2-YZn_3	- 8,110	27	6.30	0.03	735-1170
YZn_3-YZn_4	- 7,670	14	6.01	0.02	840-1100
YZn_4-YZn_5	- 8,190	40	6.78	0.04	865-1110
YZn_5-Y_2Zn_{17}	- 7,800	52	6.47	0.06	830-1115
Y_2Zn_{17}-YZn_{11}	- 6,800	29	5.87	0.04	720-960

*σ_s and σ_i are the standard deviations for the constants a and b respectively.

YZn_2 as discussed in the preceding section. Since the alloys were annealed at temperatures well above 750°C before dewpoint measurements were made and due to the high degree of supercooling required to transform the beta YZn_2 in this composition range, the beta phase was probably present throughout the temperature range for which dewpoint data were obtained.

The standard free energy of vaporization and vapor pressure of pure liquid zinc in the temperature range 692.7° to 1181°K may be represented by the relations [5]

$$\Delta F^{\circ} = 30,547 + 5.826T \log T - 43,766T \qquad (1a)$$

and

$$\log_{10} P_{atm.} = \frac{-6,678}{T} - 1.274 \log T + 9.568 \qquad (1b)$$

respectively. For the sublimation of pure solid zinc, 298° to 692.7°K, the corresponding relations are

$$\Delta F^{\circ} = 31,400 + 0.875T \log T + 1.2\times10^{-3}T^2 - 31.757T \qquad (2a)$$

and

$$\log_{10} P_{atm.} = \frac{-6,865}{T} - 0.1913 \log T - 0.262\times10^{-3}T + 6.943 \qquad (2b)$$

The vapor pressures of zinc over the alloys were calculated from the dewpoint temperatures and equation (1b). A few measurements for which the dewpoint temperatures were below the melting point of pure zinc required the use of equation (2b). The relations for the vapor pressure given in Table I

are based on vapor pressures determined from these two equations, 1b and 2b. It is possible to derive from these data the standard free energy, enthalpy and entropy of formation of the various intermetallic compounds formed. For example, considering the first two phase region in which solid Y, solid YZn and zinc vapor at P_1 are in equilibrium, the following relations can be written:

$$Y(s) + Zn(v) \longrightarrow YZn(s) \qquad \Delta F^{o} = RT\ln P_1$$

$$Zn(\ell) \longrightarrow Zn(v) \qquad \Delta F^{o} = -RT\ln P^{o}$$

$$Y(s) + Zn(\ell) \longrightarrow YZn(s) \qquad \Delta F^{o}_{I} = RT\ln \frac{P_1}{P^{o}}$$

where s, ℓ, and v refer to solid, liquid, and vapor states respectively and P^{o} is the vapor pressure of pure liquid zinc. Log P_1 is given by the first equation in Table I and log P^{o} is given by equation 1b. Combining these equations according to the relation for ΔF^{o}_{I} yields the first equation given in Table II for the standard free energy of formation for YZn. Similar relations can be written for the other two phase regions. A more detailed discussion of the above relations is given in reference 5.

Table II. Relations for the standard free energy of formation of Y-Zn compounds

$$nY(s) + mZn(\ell) \longrightarrow Y_nZn_m(s)$$

Compound	Equation
YZn	$\Delta F^o = -22{,}090 + 5.826T \log T - 11.657T$
αYZn_2	$\Delta F^o = -35{,}630 + 11.65T \log T - 24.73T$
βYZn_2	$\Delta F^o = -33{,}170 + 11.65T \log T - 27.13T$
YZn_3	$\Delta F^o = -39{,}710 + 17.48T \log T - 42.07T$
YZn_4	$\Delta F^o = -44{,}260 + 23.30T \log T - 58.36T$
YZn_5	$\Delta F^o = -51{,}160 + 29.13T \log T - 71.13T$
Y_2Zn_{17}	$\Delta F^o = -138{,}250 + 99.04T \log T - 241.31T$
YZn_{11}	$\Delta F^o = -70{,}560 + 64.09T \log T - 162.92T$

Derived relations for the standard free energy of formation of the various yttrium-zinc compounds are given in Table II. ΔH^o and ΔS^o may be obtained from the equations for ΔF^o by differentiation,

$$\frac{d(\Delta F^o/T)}{d(1/T)} = \Delta H^o, \text{ and } \frac{d\Delta F}{dT} = -\Delta S^o .$$

Values calculated from the relations in Table II for the temperatures 773, 973 and 1173^{o}K are given in Table III. The 298^{o}K values given in the same table were obtained from a consideration of the reactions

$$nY(s) + mZn(\ell) \longrightarrow Y_nZn_m(s), \qquad (a),$$

$$\underline{mZn(s) \longrightarrow mZn(\ell), \qquad (b),}$$

$$nY(s) + mZn(s) \longrightarrow Y_nZn_m(s), \qquad (c),$$

from which $\Delta F_c^o = \Delta F_a^o + \Delta F_b^o$. Relations for ΔF_a^o are given in Table II and ΔF_b^o, the standard free energy of fusion for pure zinc, may be obtained from equations 1a and 2a. ΔF_c^o represents the standard free energy of formation of the compound Y_nZn_m from pure solid yttrium and pure solid zinc. In effect this treatment assumes it is valid to extrapolate the equations in Table II to temperatures below the melting point of zinc.

In the above calculations it was assumed that the compounds are line compounds, and that the heat of vaporization

Table III. Calculated values for the standard free energy, enthalpy and entropy of formation of Y-Zn compounds

Compound	Temp. ^{o}K	$-\Delta F^{o}$ cal/mole	$-\Delta H^{o}$ cal/mole	$-\Delta S^{o}$ cal/mole ^{o}K
YZn	298	20,380	21,460	3.61
	773	18,090	24,050	7.70
	973	16,490	24,550	8.28
	1173	14,790	25,060	8.75
$YZn_2\alpha$	298	32,630	34,370	5.81
" α	773	28,730	39,540	14.0
" α	973	25,820	40,560	15.2
" β	1173	23,040	39,110	13.7
YZn_3	298	36,700	37,810	3.74
	773	33,210	45,580	16.0
	973	29,830	47,100	17.8
	1173	26,130	48,610	19.2
YZn_4	298	40,920	41,730	2.72
	773	37,340	52,080	19.1
	973	33,290	54,110	21.4
	1173	28,810	56,130	23.3
YZn_5	298	46,440	47,990	5.22
	773	41,110	60,930	25.6
	973	35,670	63,460	28.6
	1173	29,720	66,000	30.9
Y_2Zn_{17}	298	122,050	127,500	18.3
	773	103,670	171,510	87.8
	973	85,090	180,110	97.7
	1173	64,730	188,710	105.7
YZn_{11}	298	62,100	63,600	5.04
	773	53,430	92,080	50.0
	973	42,760	97,640	56.4
	1173	30,940	103,210	61.6

or sublimation of zinc from the alloys is a constant as determined from the linear relations for log P vs 1/T as given in Table I. The largest uncertainty in the calculated values arises from the latter assumption. If heat capacity data for the alloys or intermetallic compounds were available this assumption would not be necessary.

Assuming only random errors in the zinc vapor pressures determined by the dewpoint method the probable error in log P may be calculated from the relation

$$E_{(\log P)} = \left[\sigma_i^2 + \frac{\sigma_s^2}{T}\left(\frac{1}{T} - \frac{2}{T_{ave}}\right)\right]^{\frac{1}{2}} (0.675 \qquad (3)$$

where σ_i and σ_s are the standard deviations in the intercept and slope, respectively, of the log P vs 1/T relations in Table I, and $T_{ave.}$ is obtained from the average 1/T for the measurements. The probable error in log P is a minimum at $(1/T)_{ave.}$. The probable error in ΔF^o per mole of zinc vaporized is given by the relation

$$E_{\Delta F^o} = 2.303\ RT\ E_{(\log P)}. \qquad (4)$$

The probable error in the enthalpy can be calculated from the standard deviation, σ_s, for the slope of the log P equations. The errors calculated from these relations are small. An indication of the error involved can also be obtained by

considering the reaction

$$YZn_{11} \longrightarrow \tfrac{1}{2}Y_2Zn_{17} + 2.5\ Zn(\ell).$$

At the peritectic decomposition temperature 685°C (958°K) ΔF^o for the reaction should be small. The change in free energy is given by the relation

$$\Delta F^o = -2.5\ RT\ \ln\left(\frac{P}{P^o}\right)_{Zn}$$

where P is the equilibrium vapor pressure of zinc at 958°K and P^o is the vapor pressure of pure zinc at the same temperature. At this temperature the zinc liquid in equilibrium with the two compounds is 99 atom pct zinc. If the activity of zinc is taken to be 0.99 (Raoult's law) then ΔF^o for the above reaction is +53 calories. The change in free energy is also given by the relation

$$\Delta F^o = \tfrac{1}{2}\Delta F^o(Y_2Zn_{17}) - \Delta F^o(YZn_{11}).$$

The value obtained from the relations in Table II is +310 calories. The calculated activity of zinc in the zinc-rich liquid from this value for the free energy, or calculated from the vapor pressure relations, is 0.94 and the activity coefficient is 0.95. This value for the activity coefficient is probably too low and the error in the free energy is probably less than 260 calories. The probable error calculated from equation (4) is $\pm$ 150 calories.

The enthalpy change for the above reaction, assuming ideal behavior for zinc in the zinc-rich liquid, can be calculated from the change in slope of the liquidus curve as given by the solubility equations presented in the introduction. The value obtained is 13 $\pm$ 2 K calories. The value obtained from the equations in Table II is 7.5 K calories. An error of about five pct in the standard enthalpy of formation for either YZn_{11} or Y_2Zn_{17} could account for the difference in these results. The probable error in the enthalpy as calculated from the standard deviation in the slope of the log P equation, last equation in Table I, is only 225 calories.

In the temperature range of 773 to 1173^{o}K the free energy data in Table III are estimated to be within one to two percent of the true values with the higher uncertainty being associated with the free energy of formation of Y_2Zn_{17} and YZn_{11}. The uncertainty in the enthalpy data is estimated to be within five percent. The 298^{o}K entropy values of -1.0 to -2.0 entropy units per mole of alloy are certainly reasonable and are estimated to be within $\pm$ 1.0 of the true values.

ACKNOWLEDGMENTS

The authors wish to acknowledge the assistance of F. J. Rock in making electrical resistance measurements of some of the alloys investigated. D. Howell assisted in various phases of the experimental work and in the construction and maintenance of experimental apparatus. Ardis Johnson conducted all the welding operations in sealing the alloys in tantalum crucibles.

REFERENCES

1. O. N. Carlson, F. A. Schmidt and F. H. Spedding, Preparation of Yttrium Metal by Reduction of Yttrium Trifluoride with Calcium, U.S.A.E.C. Report, ISC-744, 1956.

2. Paul F. Woerner, Separation of Metals as Hydrides from Liquid Metal Solutions, Ph.D. Thesis, Iowa State University, Ames, Iowa, 1960, p. 58.

3. P. Chiotti, P. F. Woerner and S. J. S. Parry, Pyrometallurgical Reprocessing of Thorium-Uranium Fuel, Proceedings of Symposium on the Thorium Fuel Cycle, Comitato Nazionale per L'Energia Nucleare, Rome, Italy, 1961.

4. P. Chiotti and G. R. Kilp, Zinc-Zirconium System, Trans. Met. Soc. AIME, 1959, Vol. 215, p. 892.

5. P. Chiotti and K. J. Gill, Phase Diagram and Thermodynamic Properties of the Thorium-Zinc System, Trans. Met. Soc. AIME, 1961, Vol. 221, p. 573.

Table and Figure Captions

Fig. 1. Phase diagram for the yttrium-zinc system under constrained vapor conditions.

Fig. 2. Arc-melted yttrium, X150.

Fig. 3. Y-23.2 wt pct Zn eutectic, furnace cooled, Nital etch, X100.

Fig. 4. Y-42.2 wt pct Zn annealed 48 hrs at 1000°C and quenched, HNO_3 etch, showing YZn with some segregation and pptn. of yttrium, X100.

Fig. 5. Y-58 wt pct Zn, annealed 100 hrs at 910°C and quenched, HNO_3 etch, showing YZn_2 and YZn grain boundaries, X100.

Fig. 6. Same alloy as shown in Fig.5 showing twinned structure of YZn_2, polarized light, X100.

Fig. 7. Y-60.4 wt pct Zn, furnace cooled, showing acicular transformation structure of YZn_2, X500.

Fig. 8. Y-67.0 wt pct Zn, furnace cooled, HNO_3 etch, showing YZn_2 dark phase in a YZn_3 matrix, X100.

Fig. 9. Y-74.9 wt pct Zn, furnace cooled, Nital etch, showing YZn_3, light phase, in YZn_4 matrix, X100.

Fig. 10. Y-78.6 wt pct Zn, furnace cooled, Nital etch, showing one phase YZn_5, X100.

Fig. 11. Y-86.2 wt pct Zn, furnace cooled, HNO_3 etch, showing YZn_{11} in Y_2Zn_{17} matrix, X100.

Fig. 12. Y-87.9 wt pct Zn, annealed 100 hrs at 630°C, HNO_3 etch, showing Y_2Zn_{17} in YZn_{11} matrix, X100.

Fig. 13. Y-91.9 wt pct Zn, annealed 100 hrs at 630°, Nital etch, showing zinc in YZn_{11} matrix, X100.

Table I. Zinc vapor pressure as a function of temperature for yttrium-zinc alloys

$$\text{Log}_{10}P_{\text{atm.}} = a/T + b$$

Table II. Relations for the standard free energy of formation of Y-Zn compounds

$$nY(s) + mZn(\ell) \longrightarrow Y_nZn_m(s)$$

Table III. Calculated values for the standard free energy, enthalpy and entropy of formation of Y-Zn compounds

END